

A new measurement of the evolving near-infrared galaxy luminosity function out to $z \simeq 4$: a continuing challenge to theoretical models of galaxy formation

M. Cirasuolo¹, R. J. McLure¹, J. S. Dunlop^{1,2}, O. Almaini³, S. Foucaud³, C. Simpson⁴.

¹*SUPA* Institute for Astronomy, University of Edinburgh, Royal Observatory, Edinburgh EH9 3HJ*

²*Department of Physics and Astronomy, University of British Columbia, 6224 Agricultural Rd., Vancouver, B.C., V6T 1Z1, Canada*

³*School of Physics and Astronomy, University of Nottingham, University Park, Nottingham NG7 2RD*

⁴*Astrophysics Research Institute, Liverpool John Moores University, Twelve Quays House, Egerton Wharf, Birkenhead CH41 1LD*

13 October 2021

ABSTRACT

We present the most accurate measurement to date of cosmological evolution of the near-infrared galaxy luminosity function, from the local Universe out to $z \simeq 4$. The analysis is based on a large and highly complete sample of galaxies selected from the first data release of the UKIDSS Ultra Deep Survey. Exploiting a master catalogue of K - and z -band selected galaxies over an area of 0.7 square degrees, we analyse a sample of $\simeq 50,000$ galaxies, all with reliable photometry in 16-bands from the far-ultraviolet to the mid-infrared. The unique combination of large area and depth provided by the Ultra Deep Survey allows us to trace the evolution of the K -band luminosity function with unprecedented accuracy. In particular, via a maximum likelihood analysis we obtain a simple parameterization for the luminosity function and its cosmological evolution, including both luminosity and density evolution, which provides an excellent description of the data from $z = 0$ up to $z \simeq 4$. We find differential evolution for galaxies dependent on galaxy luminosity, revealing once again the “down-sizing behaviour” of galaxy formation. Finally, we compare our results with the predictions of the latest theoretical models of galaxy formation, based both on semi-analytical prescriptions, and on full hydrodynamical simulations.

Key words: galaxies: evolution - galaxies: formation - cosmology: observations

1 INTRODUCTION

In recent years outstanding progress has been made in understanding the structure and the evolution of the Universe. In particular, the canonical Lambda cold dark matter (ΛCDM) cosmological model now provides a solid framework and is able to explain a large variety of observations: from the fluctuations in the cosmic microwave background radiation (CMB) to the large scale structure of the Universe (e.g. Perlmutter et al. 1998; Riess et al. 1998; Tegmark et al. 2004; Spergel et al. 2003, 2007). Moreover, the ΛCDM model also provides a clear picture for the composition of the Universe, with baryonic matter contributing only $\simeq 4\%$ to the density and the Universe being dominated by dark energy and dark matter. Over the last fifteen years, enormous improvements in numerical N-body simulations have allowed

the hierarchical growth of the dark matter (DM) to be accurately traced, from the initial perturbations to the large scale structure we see in the local Universe (e.g. see Springel et al. 2005). However, while the evolution of the DM is now well understood, understanding the physics involved in the evolution of the baryons is much more complex. While the evolution of the DM is only subject to gravity, many other physical processes must be taken into account to describe the formation and evolution of galaxies: e.g. gas cooling, star-formation, production of dust and metals and feedback from supernovae and nuclear black holes.

Various theoretical models have been developed either by implementing semi-analytical prescriptions for the transformation of gas into stars on the DM merger tree (e.g. Kauffmann et al. 1993; Cole et al. 2000, Somerville et al. 2001) or by solving a full set of hydrodynamical equations for the DM and baryons with smooth particle hydrodynamics (SPH) simulations (e.g. Nagamine et al. 2000, 2001; Springel

* Scottish Universities Physics Alliance

& Hernquist 2003). Over the last decade, these theoretical models have become increasingly successful in some regards in explaining the observed properties of galaxies in the local Universe. Traditionally, however, most semi-analytical models have demonstrated a tendency to predict very few old/massive galaxies at high redshift ($z \gtrsim 1$) because, in the hierarchical growth of DM, large structures naturally form late by continuous merging of smaller haloes (e.g. Cole et al. 2000; Menci et al. 2002). However, this hierarchical behaviour seems to be in contrast with recent observational results, with the advent of recent near-infrared surveys, in particular, revealing the presence of a substantial population of old, massive evolved galaxies (Extremely Red Objects, Distant Red Galaxies) at $z \gtrsim 1.5$, which were previously missed by optical surveys (Cimatti et al. 2002; Daddi et al. 2002).

Several deep multi-wavelengths surveys are now ongoing or have just been completed (Cimatti et al. 2002; Giavalisco et al. 2004; Rix et al. 2004; Lawrence et al. 2007; Scoville et al. 2007) with the aim of tracing the assembly history of galaxies. Exploiting the near-infrared data and supported by spectroscopic and photometric redshift estimations, several studies have attempted to derive the evolution of the near-infrared luminosity function (LF), as a tracer of the mass assembly history of galaxies. In fact, it has long been understood that observations of the rest-frame near-infrared emission of galaxies is the best tracer of the stellar mass because it is less affected by dust absorption and ongoing star-formation (e.g. Lilly & Longair 1984; Dunlop et al. 1989; Glazebrook et al. 1995; Cowie et al. 1996; Poggianti 1997).

Several authors have found evidence for evolution of the near-infrared LF with redshift, with the evolution being very slow from the local Universe up to $z \sim 0.5$ and then progressively faster (Glazebrook et al. 1995; Bolzonella et al. 2002; Pozzetti et al. 2003; Dickinson et al. 2003; Drory et al. 2003; Caputi et al. 2006; Saracco et al. 2006). However, as shown by Saracco et al., there are still some discrepancies between results obtained by different authors, especially at the bright end, presumably due to the small-number statistics imposed by the limited areal coverage of the available data. Recently, the advent of the Spitzer satellite has provided the opportunity to derive reliable estimates for the stellar masses in galaxies at high redshift, allowing a direct study of the evolution of the mass function (Fontana 2004, 2006; Drory et al. 2005; Perez-Gonzalez et al. 2008; Pozzetti et al. 2007). These studies have consolidated the “downsizing” scenario (Cowie et al. 1996) in which the more massive galaxies form their stars at higher redshift and on a shorter time scale compared to less massive systems.

From the theoretical point of view, this apparent discrepancy between the hierarchical growth of DM and the downsizing evolution observed in galaxies seems to be reconciled in the latest models by properly taking into account both stellar and nuclear feedback (Granato et al. 2001, 2004; Cirasuolo et al. 2005; Di Matteo et al. 2005; Croton et al. 2006; Bower et al. 2006; Menci et al. 2006; Monaco et al. 2007).

The aim of this work is to obtain an extremely accurate determination of the cosmological evolution of the near-infrared galaxy LF which can then be wielded as a powerful tool to constrain and possibly discriminate between the var-

ious prescriptions for the physical mechanisms implemented in galaxy-formation models.

The layout of the paper is as follows. In Section 2 we summarize the main properties of the datasets used in this work and in Section 3 we describe in detail the method we have developed for the estimation of redshifts from the available multi-band photometry. In Section 4 we derive the near-infrared LF and its cosmological evolution, comparing it with previous results found in literature. Finally in Section 5 we compare our results with the predictions of some of the latest models of galaxy formation. Our conclusions are presented in Section 6.

Throughout this paper all magnitudes are quoted in the AB system (Oke & Gunn 1983) and we have adopted a concordance cosmology with $\Omega_M = 0.3$, $\Omega_\Lambda = 0.7$ and $H_0 = 70 \text{ km s}^{-1}$.

2 THE DATA-SETS

The aim of this paper is to analyse the evolutionary properties of galaxies by exploiting the Ultra Deep Survey (UDS), the deepest of the five surveys that constitute the UKIRT Infrared Deep Sky Survey (UKIDSS - Lawrence et al. 2007). For the purpose of this work we used data from the first data release of the survey (DR1; Warren et al. 2007), which includes imaging in the J - and K -bands with 5σ depths of 23.3 and 23.1 respectively within a 3-arcsec diameter aperture. Crucially, the UDS field benefits from a large area (0.8 square degrees) and deep multi-wavelength coverage. For this work we primarily exploit the deep optical data from the Subaru XMM-Newton Deep Survey (SXDS; Sekiguchi et al. 2005; Furusawa et al. 2008), which covers most of the UDS field in $BVRi'z'$ filters to typical 5σ depths of $B = 27.5$, $V = 26.7$, $R = 27.0$, $i' = 26.8$ and $z' = 25.9$ (within a 3-arcsec diameter aperture).

For the construction of the initial galaxy catalogue we performed source extraction on the K -band mosaic by using the public code `SEXTRACTOR` (Bertin & Arnout 1996). The number counts for the K -band selected sources are shown in Fig. 1 and compared with previous estimates found in the literature. In order to improve the completeness of our sample at faint magnitudes, we also performed source extraction on the z' -band images from the SXDS. The advantage of doing this is that the z' -band images are ~ 2.5 magnitudes deeper than the DR1 K -band data in the UDS. Therefore, performing aperture photometry on the K -band images centered at the position of the z' -band extracted sources allowed us to increase the completeness close to the K -band flux limit, at least for sources which do not have extremely red colours (e.g. $z' - K < 2$).

This technique allowed us to build a *master-catalogue* including all the sources extracted directly from the K -band images, plus all the sources selected in the z' -band with a counterpart in the K -band mosaic. The number counts for sources in the master-catalogue ($K + z'$ selected) are shown in Fig. 1 with filled dots. As can be seen from Fig. 1, the procedure of selecting sources in both the K - and z' -bands has increased the completeness of the sample to $\simeq 100\%$ at $K \leq 23$.

To fully exploit the high completeness of our sample, for the purpose of this work we only considered sources in

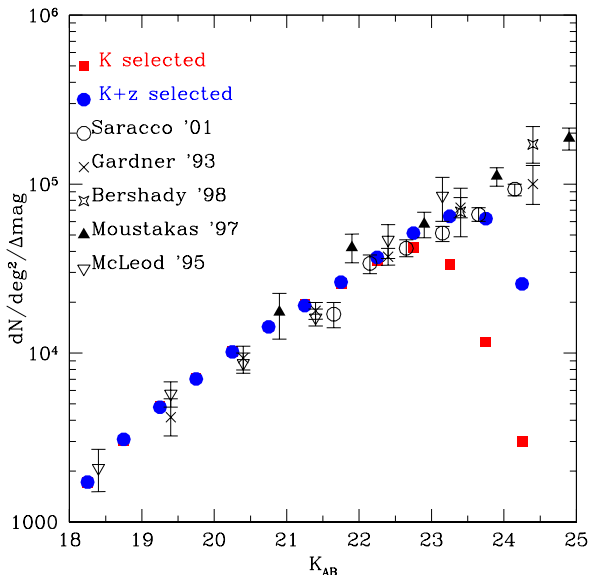


Figure 1. Number counts in the K -band for sources in the UDS field. The K -band selected (solid squares) and $K + z'$ selected (filled dots) samples are described in the text. For comparison we also show the number counts in the K -band from Saracco et al. (2001, open circles), Gardner et al. (1993, crosses), Bershady et al. (1998, stars) Moustakas et al. (1997, filled triangles), and McLeod et al. (1995, open triangles).

the master-catalogue with $K \leq 23$ and limit the analysis to an area of 0.7 square degrees which is covered by both the UDS and SXDS imaging. In order to model the spectral energy distribution (SED) of these sources, we performed aperture photometry on the $BVRiz'JK$ images centered at the position of the $K + z'$ selected sources. The optical and near-infrared photometry were measured in $3''$ diameter apertures, and then point spread function (PSF) corrected to total magnitudes. The consistent image quality of the optical and near-infrared data, with Full Width Half Maximum (FWHM) in the range $0.75 < \text{FWHM} < 0.80$ arcsec, means that the differential aperture corrections between bands are small (≤ 0.1 mag).

The UDS field also benefits from optical data obtained with the Canada-France-Hawaii telescope (CFHT) as part of the CFHT Legacy Survey. Source catalogues in u, g, r, i, z bands from the TERAPIX release 3 (T0003) were retrieved from the CFHT legacy survey website¹ and matched with the sources in the master catalogue by using a searching radius of 1 arcsec. The typical 5σ depths for the CFHT data (MAGAUTO) are: $u = 25.3$, $g = 25.2$, $r = 24.7$, $i = 24.4$ and $z = 22.5$.

Extremely valuable coverage of the UDS at mid-infrared wavelengths is provided by the *Spitzer* satellite as part of the *Spitzer* wide-area infrared extragalactic (SWIRE) survey (Lonsdale et al. 2003; 2004). For the present study we exploited the IRAC data at $3.6\mu\text{m}$ and $4.5\mu\text{m}$ presented in the second data release (Surace et al. 2005). We performed aperture photometry on the IRAC images centered at the

position of the $K + z'$ -selected sources within a $3''$ -diameter aperture. Since the mean FWHM of the IRAC PSF at $3.6\mu\text{m}$ is 1.66 arcsec (Fazio et al. 2004) the magnitudes required aperture correcting to match the total magnitudes. We performed tests studying the curve of growth of isolated stars in the field and derived aperture corrections of 0.53 and 0.58 magnitudes for the $3.6\mu\text{m}$ and $4.5\mu\text{m}$ channels respectively, in agreement with Surace et al. (2005).

At shorter wavelengths the available multi-wavelength data in the UDS has recently been complemented by observations in the ultraviolet obtained with the *GALEX* satellite (both FUV and NUV channels). Given the large FWHM of the *GALEX* PSF ($6''$) we used the total magnitudes given in the *GALEX* archive catalogues² and matched sources by using a searching radius of 2 arcsec.

Star-galaxy separation has been performed by combining information from the stellarity parameter, as measured by *SExtractor* on the SXDS images, with the position of the sources in the BzK colour-colour diagram (Daddi et al. 2004). As pointed out by Daddi et al., stars have colours that are clearly separated from the region occupied by galaxies and can be efficiently isolated with the criterion $(z' - K) < 0.3(B - z') - 0.5$. It is worth noting that the vast majority of these sources classified as stars also show an unacceptable value of the χ^2 when fitted with galaxy templates.

To summarise, the master-catalogue of sources we used for this work has been selected by using both the UKIRT WFCAM K -band and Subaru SuprimeCam z' -band images in the UDS field. For the following analysis we consider $\approx 50,000$ sources with $K \leq 23$ over an area of 0.7 square degrees, with each source having reliable photometry (detections or upper-limits) in 16 broad-bands from the far-ultraviolet to $4.5\mu\text{m}$.

3 REDSHIFT DETERMINATION

The extensive and deep multi-wavelength information in the UDS field is vital for detailed modelling of the galaxy spectral energy distributions (SEDs). Following Cirasuolo et al. (2007), we derived photometric redshifts for all the sources in the $K + z'$ master catalogue by fitting the observed photometry with both empirical and synthetic galaxy templates.

3.1 Photometric redshifts

The fitting procedure to derive photometric redshifts, based on χ^2 minimization, was performed with a code based largely on the public package *Hyperz* (Bolzonella, Miralles & Pelló 2000). As empirical templates we used both the average local galaxies SEDs derived by Coleman, Wu and Weedman (CWW) and the more recent templates obtained within the K20 survey (Cimatti et al. 2002; Mignoli et al. 2005). In order to improve the characterization of young, blue galaxies we also implemented six SEDs of observed starbursts from Kinney et al. (1996).

To generate synthetic templates of galaxies we used

¹ <http://www.cfht.hawaii.edu/Science/CFHLS/>

² <http://galex.stsci.edu/GR1/>

the stellar population synthesis models of Bruzual & Charlot (2003) assuming a Salpeter initial mass function (IMF) with a lower and upper mass cutoff of 0.1 and 100 M_{\odot} respectively. We used a variety of star-formation histories; instantaneous-burst and exponentially-declining star formation with e -folding times $0.3 \leq \tau(\text{Gyr}) \leq 15$, all with a fixed solar metallicity. Dust reddening was taken into account by following the obscuration law of Calzetti et al. (2000) within the range $0 \leq A_V \leq 2$. We also added a prescription for the Lyman series absorption due to the HI clouds in the inter galactic medium, according to Madau (1995). Finally, at each redshift, we only permitted models with an age less than the age of the Universe at that redshift.

3.2 Spectroscopic redshifts

The UDS also benefits from various large spectroscopic campaigns that allow us to test the reliability of our redshift estimations. Fig. 2 shows the comparison of our photometric redshifts estimates for ~ 1200 galaxies in the UDS field with secure spectroscopic redshifts (Yamada et al. 2005; Akiyama et al. in preparation; Smail et al. in preparation; Simpson et al. 2006a). The agreement is remarkably good over the full redshift range $0 < z < 6$. The fraction of outliers (defined as sources with $|\Delta z|/(1+z) \equiv |(z_{\text{spect}} - z_{\text{phot}})|/(1+z_{\text{spect}}) > 0.15$) is extremely low, less than 2%. The improvement compared with our previous work (Cirasuolo et al. 2007) is mainly due to the added value of the u -band and Galax data, which significantly helps to remove the degeneracy between double minima in redshift space.

More quantitatively, the accuracy of our photometric redshifts can be estimated by looking at the distribution of the $\Delta z/(1+z)$ as shown in the small inset in Fig. 2. The distribution has a mean consistent with zero (0.008) and a standard deviation $\sigma = 0.034$ (excluding the few outliers with $|\Delta z|/(1+z) > 0.15$). This accuracy is comparable to the best available from other surveys such as GOODS and COSMOS (Caputi et al. 2006; Grazian et al. 2006; Mobasher et al. 2007). As already pointed out in our previous work (Cirasuolo et al. 2007), this accuracy is preserved down to faint K -band magnitudes ($K \geq 22$) and up to very high redshifts ($z > 5$). The ongoing large spectroscopic campaign (PI Almaini) with the Very Large Telescope to observe galaxies in the UDS with both VIMOS and FORS2 will, in the near future, allow us to further test and refine our results.

4 LUMINOSITY FUNCTION

Building on the reliable SED fitting procedure described previously, in this Section we exploit our large sample of UDS galaxies to characterise the evolution of the rest-frame near-infrared LF. Following Cirasuolo et al. (2007), the rest-frame absolute K -band magnitudes have been computed by using the closest observed band to the rest-frame K -band depending on the redshift of the source. This method in fact minimises the uncertainties related to the k -corrections.

The rest-frame K -band LF in the redshift range $0.2 \lesssim z \lesssim 4$ has been computed by using two independent methods: the $1/V_{\text{max}}$ method (Schmidt 1968) and the maximum likelihood analysis of Marshall et al (1983). Our results are

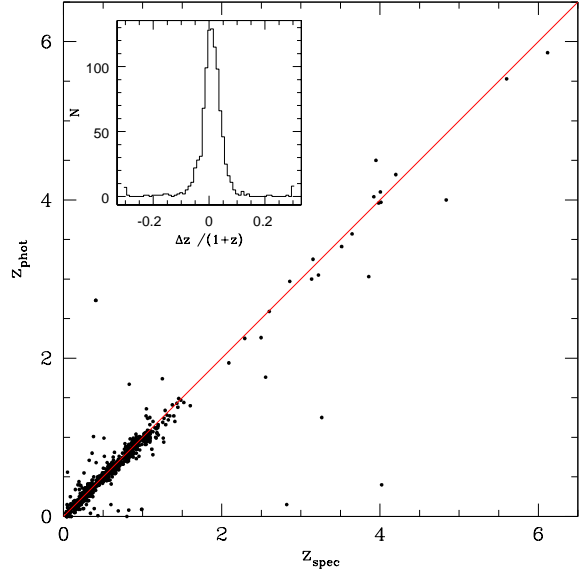


Figure 2. Photometric redshift plotted versus spectroscopic redshift for ~ 1200 galaxies in the UDS sample with secure spectroscopic redshifts (Yamada et al. 2005; Akiyama et al. in preparation; Smail et al. in preparation; Simpson et al. 2006a; Simpson et al. in preparation). The small inset shows the distribution of $\Delta z/(1+z)$. The agreement is remarkably good; the mean value of the distribution of $\Delta z/(1+z)$ is 0.008, with a standard deviation $\sigma = 0.034$, excluding the clear outliers (see text for details).

shown in Fig. 3. The LF in twelve redshift intervals computed via $1/V_{\text{max}}$ method is shown in the figure as solid dots. The error-bars on the determination of the space density of sources in each redshift and magnitude bin account for both Poissonian statistical errors and the uncertainty in the photometric redshifts. The latter has been estimated by reconstructing several LFs, perturbing the value of the photometric redshift within its 1σ confidence interval. For each source the SED-fitting procedure provides the best-fit redshift (identified by the lowest value of the χ^2) and the 1σ interval defined as the redshift space around the best-fit minimum with $\Delta\chi^2 \equiv \chi_z^2 - \chi_{\text{min}}^2 \leq 1$ (marginalising over the other free parameters in the SED fitting e.g. age, reddening etc.). We performed Monte Carlo realizations, with each source being allocated a random value for its redshift within its 1σ confidence interval, and having its luminosity recomputed appropriately before reconstructing the LF. The errors reported in Fig. 3 reflect the maximum differences in the LF obtained from these different realizations.

An independent estimation of the LF has been obtained by using the maximum likelihood analysis. This method is less biased by strong density inhomogeneity in the field, compared to the $1/V_{\text{max}}$ method, but requires an *a priori* assumption regarding the shape of the LF. This latter has been parameterised with a Schechter function (Schechter 1976):

$$\phi(M) = 0.4 \ln(10) \phi_0 10^{-0.4 \Delta M (\alpha+1)} \exp(-10^{-0.4 \Delta M}) \quad (1)$$

with $\Delta M = M_K - M_K^*$ assuming both a luminosity and density evolution with redshift parameterised as:

$$M_K^*(z) = M_K^*(z=0) - \left(\frac{z}{z_M}\right)^{k_M}, \quad (2)$$

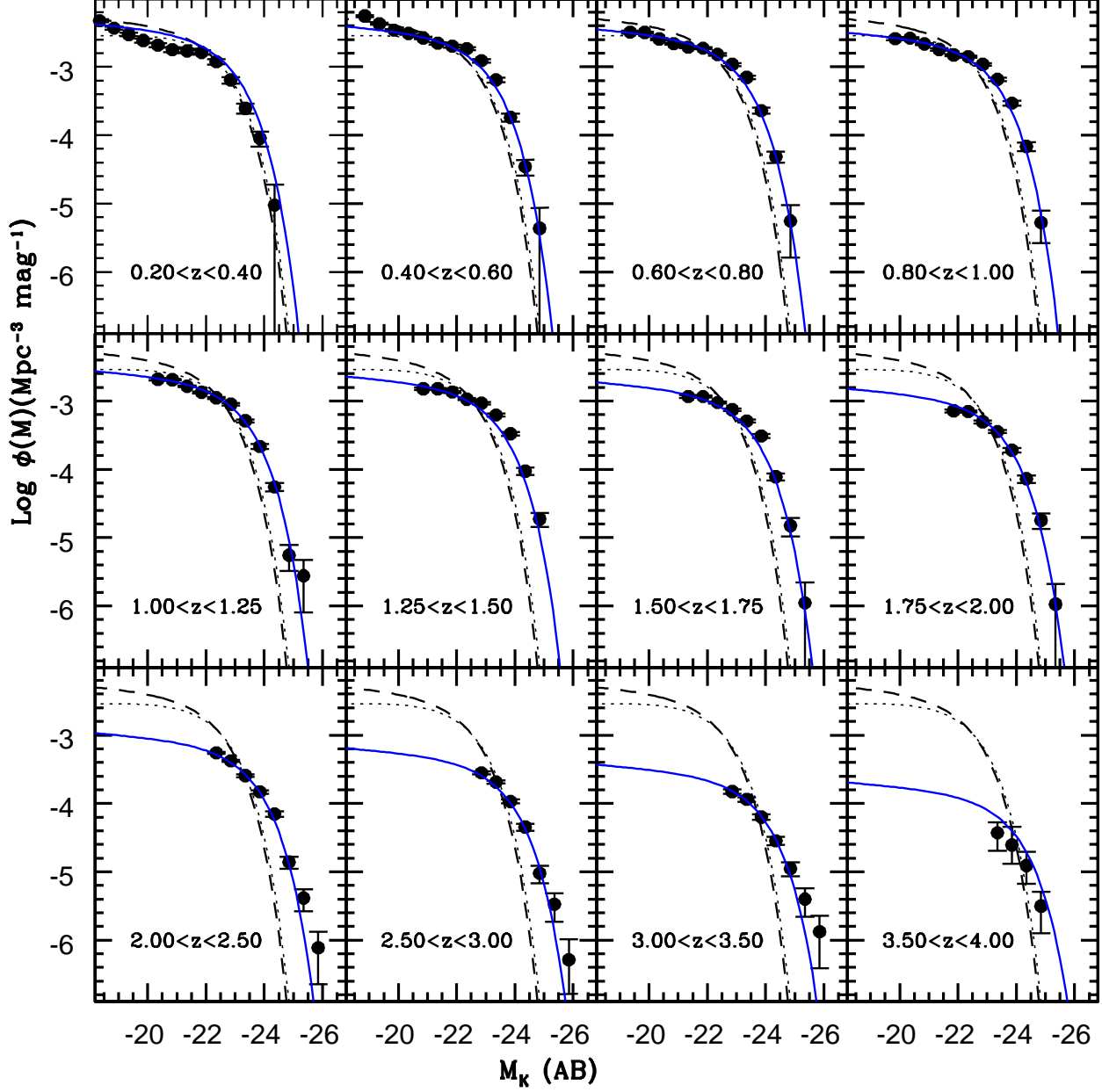


Figure 3. Rest-frame K -band luminosity function in twelve redshift bins in the range $0.2 \leq z \leq 4$. The solid dots represent the LF obtained with the $1/V_{max}$ method for sources in the UDS sample, while the solid line is the best fit Schechter function obtained from the likelihood analysis and plotted at the mean redshift of each bin. For comparison, the dashed and dotted lines are the LFs at $z = 0$ obtained by Kochanek et al. (2001) and Cole et al. (2001), respectively.

$$\phi_0(z) = \phi_0(z=0) \times \exp \left[- \left(\frac{z}{z_\phi} \right)^{k_\phi} \right] \quad (3)$$

The local value of the characteristic luminosity, $M_K^*(z=0)$, has been fixed to match the local value -22.26 ± 0.05 (converted to AB using $K_{AB} = K_{Vega} + 1.9$ and using $h = 0.7$) derived by Kochanek et al. (2001) from the Two Micron All Sky Survey (2MASS). It is worth noting that this value is

very close to the value -22.31 ± 0.03 derived by Cole et al. (2001). The maximum likelihood analysis was performed by minimizing over the other five free parameters: the faint end slope α and four parameters (z_M, k_M, z_ϕ, k_ϕ) describing the evolution with redshift. The best fit values for these parameters are given in Table 1, along with the overall normalization at redshift zero, $\phi_0(z=0)$, obtained *a posteriori* by fitting the observed number counts. It is reassuring that

Table 1. Best fit parameters for the Schechter LF and its redshift evolution.

α	-1.07 ± 0.1
$M_K^*(z=0)$	-22.26 (fixed)
z_M	1.78 ± 0.15
k_M	0.47 ± 0.2
z_ϕ	1.70 ± 0.09
k_ϕ	1.47 ± 0.1
$\phi_0(z=0)$	$(3.5 \pm 0.4) \times 10^{-3}$ (Mpc $^{-3}$)

the value of $\phi_0(z=0)$ we obtain is in excellent agreement with the local value of 0.0039 Mpc $^{-3}$ and 0.0037 Mpc $^{-3}$, derived by Kochanek et al (2001) and Cole et al. (2001), respectively.

First of all it is worth noting the excellent agreement between the estimation of the LF obtained with the two independent methods ($1/V_{\max}$ and maximum likelihood) as shown in Fig. 3. The large sample of galaxies provided by the UDS has allowed us to split the LF into narrow redshift and magnitude bins, while still preserving high statistical significance.

As a further check of the reliability of our results we find our estimate of the LF to be consistent with previous studies published in the literature. In Fig. 4 we show the comparison with results obtained by Pozzetti et al. (2003) from the K20 survey, Caputi et al. (2006) from the Great Observatories Origins Deep Survey (GOODS) / Chandra Deep Field South (CDFs), and Saracco et al. (2006) from the Hubble deep field south (HDF-S). In particular, Saracco et al. exploited the very deep near-infrared observations of the HDF-S (FIRES, Franx et al. 2003) down to $K \leq 24.9$ to derive an estimate of the faint end of the LF up to $z \sim 3$. They found the value of the slope of the LF to be unchanged with redshift, consistent with the results we have obtained here from the maximum-likelihood analysis ($\alpha \simeq -1$). The small discrepancy in the normalization at $z \simeq 2$ between our LF and the one estimated by Saracco et al. can be ascribed to the fact that their LF is actually computed over a wider redshift range $1.9 \leq z \leq 4$, whereas we have simply plotted the LF at $z \simeq 2.5$.

Overall our estimate of the LF is in good agreement with previous results. However, the much larger statistics provided by the UDS dataset has produced a substantial improvement in the determination of the LF and its cosmological evolution. As clearly shown in Fig. 3, the unique combination of area and depth provided by the UDS allows the evolution of the LF, and in particular the bright end of the LF, to be accurately traced out to $z \geq 3$. In fact, the large increase in the areal coverage compared to previous studies – more than a factor 16 compared to the CDFs and a factor of nearly 400 larger than the HUDF-FIRES – has allowed us to trace the evolution of rare, bright/massive galaxies with unprecedented accuracy.

The maximum-likelihood analysis and the direct comparison of our results with the local K -band LF obtained by Kochanek et al. (2001) and Cole et al. (2001) suggest a combination of luminosity and density evolution for the LF with cosmic time. In agreement with previous studies (Pozzetti et al 2003; Drory et al. 2003; Feulner et al. 2003;

Caputi et al. 2006; Saracco et al. 2006; Cirasuolo et al. 2007) we confirm the substantial brightening of the characteristic luminosity by $\simeq 1$ magnitude from $z = 0$ to $z \simeq 2$ and an overall decrement in the total normalization by a factor $\simeq 3.5$ over the same redshift interval. Given the exponential tail of the bright end of the LF the net result of this combined luminosity and density evolution is that the space density of the brightest sources with $M_K \simeq -24$ rapidly increases from the local Universe up to $z \simeq 1$ and then stays roughly constant up to $z \simeq 2$, with a mild decline at higher redshift (see Fig. 5). This suggests that a large population of very bright/massive galaxies have assembled the bulk of their stars at high redshift, in the range $1 \lesssim z \lesssim 3$. On the other hand the sharp decline in the space density of these bright systems at $z \lesssim 1$ is mainly due to the fading of the characteristic luminosity M_K^* , consistent with the passive evolution of a single stellar population as shown in Cirasuolo et al. (2007). This strongly suggests that, by $z \simeq 1$, massive galaxies have terminated their mass assembly phase and that their luminosities then proceed to fade passively with cosmic time.

The evolutionary behaviour of less-luminous objects is somewhat different. As shown in Fig. 5 the space density of galaxies with intermediate luminosity $M_K \simeq -22$ (the local value of the characteristic luminosity M_K^*) is roughly constant up to $z \simeq 1$, but then decreases by more than a factor of 5 by $z \simeq 3$. The evolution of less luminous galaxies (e.g. $M_K \simeq -20$) is even more rapid, with a decline in the space density of a factor ~ 2 already apparent by $z \simeq 1$ and by more than a factor 4 at $z \simeq 2$. It is worth noticing that in this latter case, with the current sample, we can only directly trace the very faint sources with $M_K \simeq -20$ out to $z \sim 1.2$. At higher redshift we rely on the extrapolation at low luminosities of the LF given by the maximum likelihood analysis, but, as shown in Fig. 4, the faint-end slope of the LF at these redshifts is consistent with the results obtained by Saracco et al. (2006).

5 COMPARISON WITH PREDICTIONS OF THEORETICAL MODELS

The presence of a large population of massive galaxies at high redshift has presented a major challenge for models of galaxy formation. In fact, models able to reproduce the local luminosity function have often largely under-predicted the number of bright/massive galaxies at high redshift (White & Frenk 1991; Kauffmann et al. 1993; Cole et al. 2000; Menci et al. 2002). On the other hand, models tuned to create more massive systems at high redshift have struggled to prevent further cooling flows and the continuous growth of these systems, resulting in an over-prediction of massive systems in the local Universe (Kauffmann et al. 1999a,b).

The mutual feedback between star formation and accretion onto the central black hole has proven to be very effective in solving this problem. The energy injected into the system by nuclear activity is able to quench star-formation and expel the remaining cold gas from the galaxy (see Ciotti & Ostriker 1997; Silk & Rees 1998; Fabian 1999). This nuclear feedback was first successfully introduced into a cosmological framework of galaxy formation by Granato et al. (2001, 2004) and then implemented by many other authors

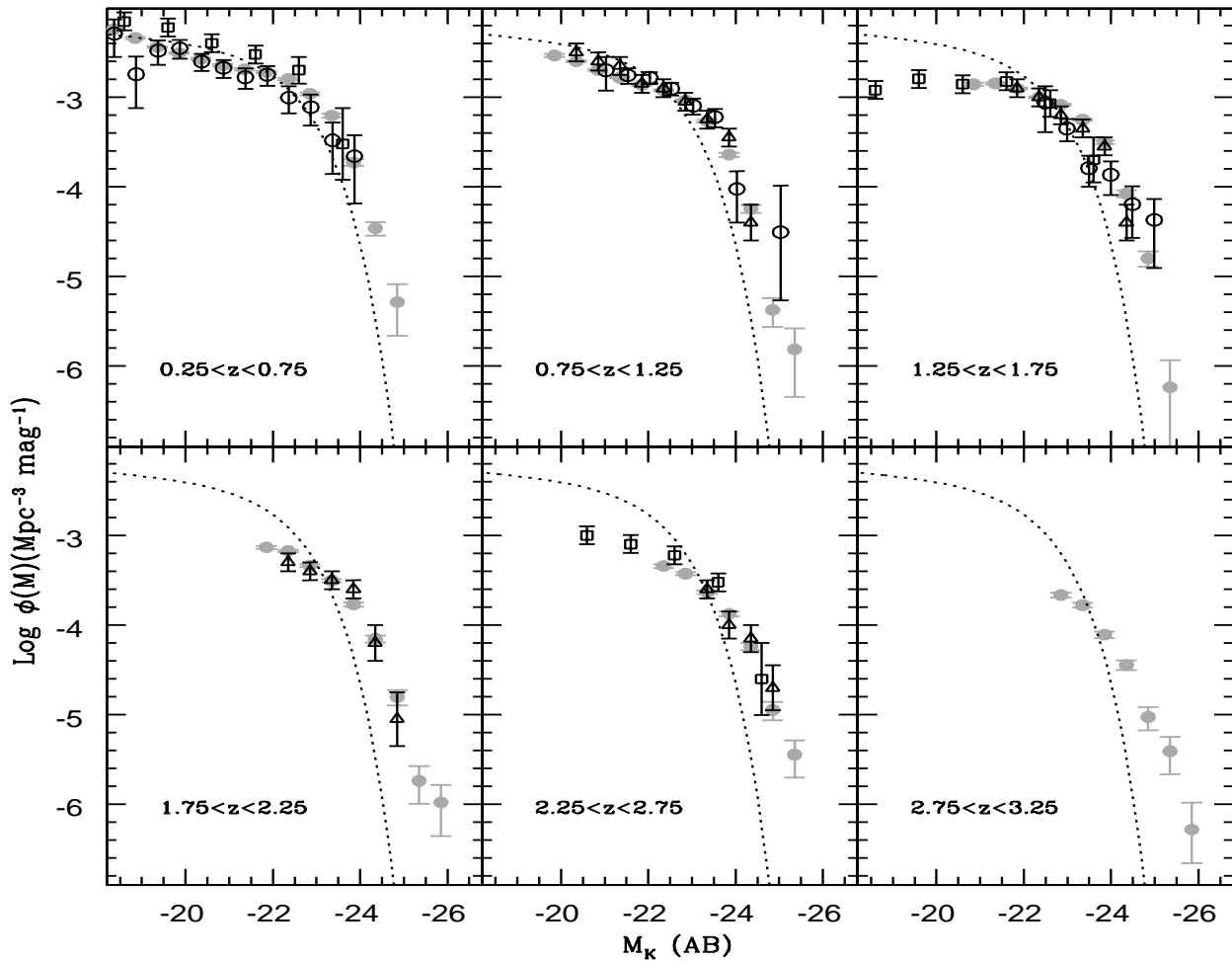


Figure 4. Comparison of our estimation of the K -band LF (solid gray dots) with previous results found in the literature. Open circles show the LF obtained by Pozzetti et al. (2003) from the K20 survey, open triangles are the Caputi et al. (2006) results from the GOODS/CDFS and open squares illustrate the estimates obtained by Saracco et al. (2006) from the HDF-S. The dotted line is the local luminosity function of Kochanek et al. (2001).

(e.g. Di Matteo et al. 2005; Croton et al. 2006; Bower et al. 2006; Menci et al. 2006; Monaco et al. 2007).

In this section we compare our results with the predictions of some of the latest models of galaxy formation, most of them including some kind of recipe for active galactic nuclei (AGN) feedback.

Firstly, we considered two semi-analytical models by Bower et al. (2006) and De Lucia & Blaizot (2007) which implement the physics of baryonic collapse, growth of the central black hole and feedback from supernovae and AGN on the Millennium simulation of the growth of the dark matter structures in the Λ CDM cosmology (Springel et al. 2005).

Both models implement feedback from nuclear activity to quench cooling flows and regulate the formation of massive systems. Even though they utilise different prescriptions (described in Bower et al. 2006 and Croton et al. 2006), both models assume the nuclear feedback to be driven by low-energy radio activity (the so-called “radio mode”) which occurs at low accretion rates and is found to be effective if

the gas is in quasi hydrostatic conditions, particularly at low redshift.

We also considered two other semi-analytical models which implement a rather different treatment for the AGN feedback. Menci et al. (2006) present a model in which star-formation and BH growth is triggered by galaxy encounters, both merging and fly-by. In this model the nuclear feedback is produced during the short AGN phase, where a blast wave from the central region is able to sweep the cold gas content of the galaxy on a shorter time scale and at higher redshift compared to the “radio mode” used by Bower et al. (2006) and Croton et al. (2006).

A similar “quasar mode” feedback, in which the radiation pressure from the nuclear activity blows out the cold gas from the galaxy has been adopted by Monaco et al. (2007) and Fontanot et al. (2008). They have also implemented a revised treatment for the radiative cooling of the shocked gas and feedback from galactic winds and superwinds.

Finally, we compared our results with the predictions

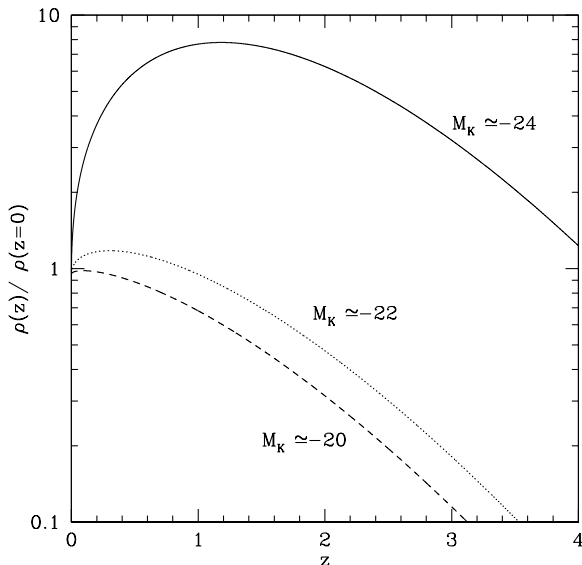


Figure 5. Evolution of the space density of sources with different rest-frame K -band luminosities as derived from the maximum-likelihood analysis and normalised to their corresponding local value.

obtained with fully hydrodynamic simulations in a cosmological context by Nagamine et al. (2006) and Cen & Ostriker (2006). These simulations use a different approach from semi-analytical models, since they solve a full set of hydro-dynamical equations for the evolution of dark matter and baryons simultaneously. These simulations implement the standard equations of gravity, hydrodynamics and atomic physics, radiative transfer, heating and cooling of the gas and supernovae feedback.

As shown in Fig. 6, the new generation of theoretical models are better able to reproduce the overall shape of the LF compared to previous models (Kauffmann et al. 1993; Cole et al. 2000; Menci et al. 2002). In particular, the inclusion of the feedback from the central BH improves the quenching of star-formation in bright, massive systems, better reconciling the predicted bright end of the LF with the observations.

However, even though there is a broad consistency – in particular with the prescriptions given by Bower et al. – the large fraction of bright galaxies already in place at high redshift is still challenging for the semi-analytical models. Especially at the highest redshifts, some of the models still predict far fewer bright galaxies than are observed. It is worth noticing that the predictions from De Lucia & Blaizot (2007), Monaco et al (2007), Menci et al. (2006) and Nagamine et al. (2006) all include a correction for attenuation by dust, which is of course more realistic but introduces more uncertainties in the predicted LF, in particular at the bright end.

On the other hand, the hydrodynamical simulations tend to over-predict the number of massive galaxies at any redshift. This could be due both to resolution effects and to a lack of feedback from the central AGN. When the resolution is not sufficient, galaxies tend to over-merge in high-density regions. The other issue is that the current hydrodynamical

simulations do not yet include explicit implementation of AGN feedback, which has proven to be very effective in suppressing the bright end of the luminosity/mass function.

It is interesting to notice that most of the models are able to reproduce well the space density of galaxies at the knee of the LF, but they consistently over-predict the space density of low-luminosity objects. This is probably due to very inefficient star formation in low-mass systems. In fact, from the modelling perspective, the feedback from AGN becomes negligible in these low-mass systems, and reducing the star-formation efficiency parameter also dramatically reduces the amount of feedback. This makes the discs gas rich and prone to low, but continuous, star-formation. This results in the over-prediction of the number of low-mass systems actually observed. Interestingly, the modelling of the star formation in the hydrodynamical simulation, at least around $z \simeq 1$, seems to be able to reproduce the shape of the faint end of the LF, offering some promise that the problem of the excess of low-luminosity sources can be resolved.

6 DISCUSSION AND CONCLUSIONS

We have presented new results on the cosmological evolution of the near-infrared galaxy luminosity function from the local Universe up to $z \simeq 4$. The analysis is based on a large and highly-complete sample of galaxies selected from the first data release of the UKIDSS Ultra Deep Survey. Exploiting a master catalogue of K - and z' -selected galaxies over an area of 0.7 square degrees, we analysed a sample of $\simeq 50,000$ galaxies, all of which possess reliable photometry in 16 bands from the far-ultraviolet to the mid-infrared. This large multi-wavelength coverage has allowed us to obtain accurate photometric redshifts and reliable estimates of rest-frame K -band luminosities up to high redshift.

The near-infrared LF and its cosmological evolution has been derived by using two independent methods ($1/V_{max}$ and maximum likelihood) and the errors computed taking into account the uncertainties in the photometric redshift estimation. In particular, via the maximum-likelihood analysis we obtained a simple parameterization for the LF and its cosmological evolution which provides an excellent description of the data from $z = 0$ up to $z \simeq 4$.

The unique combination of large area and depth offered by the UDS has allowed us to trace the evolution of the LF with unprecedented accuracy. In agreement with previous studies, we find the evolution of the LF to be well described by a combination of luminosity and density evolution. Given the shape of the LF this results in a differential evolution of galaxy number density, dependent on galaxy luminosity, and reveals once again the downsizing behaviour of galaxy formation. Bright/massive galaxies are assembled at high redshift ($1 \lesssim z \lesssim 3$) and then they passively evolved over the last few billion years, while the formation of intermediate and low luminosity objects is progressively shifted to lower redshifts.

This anti-hierarchical behaviour is broadly reproduced by most of the latest generation of theoretical models of galaxy formation. In this work we compared our observational results with the predictions of both semi-analytical models (Bower et al. 2006; De Lucia & Blaizot 2007; Monaco et al. 2007; Menci et al. 2006) and hydrodynamical simula-

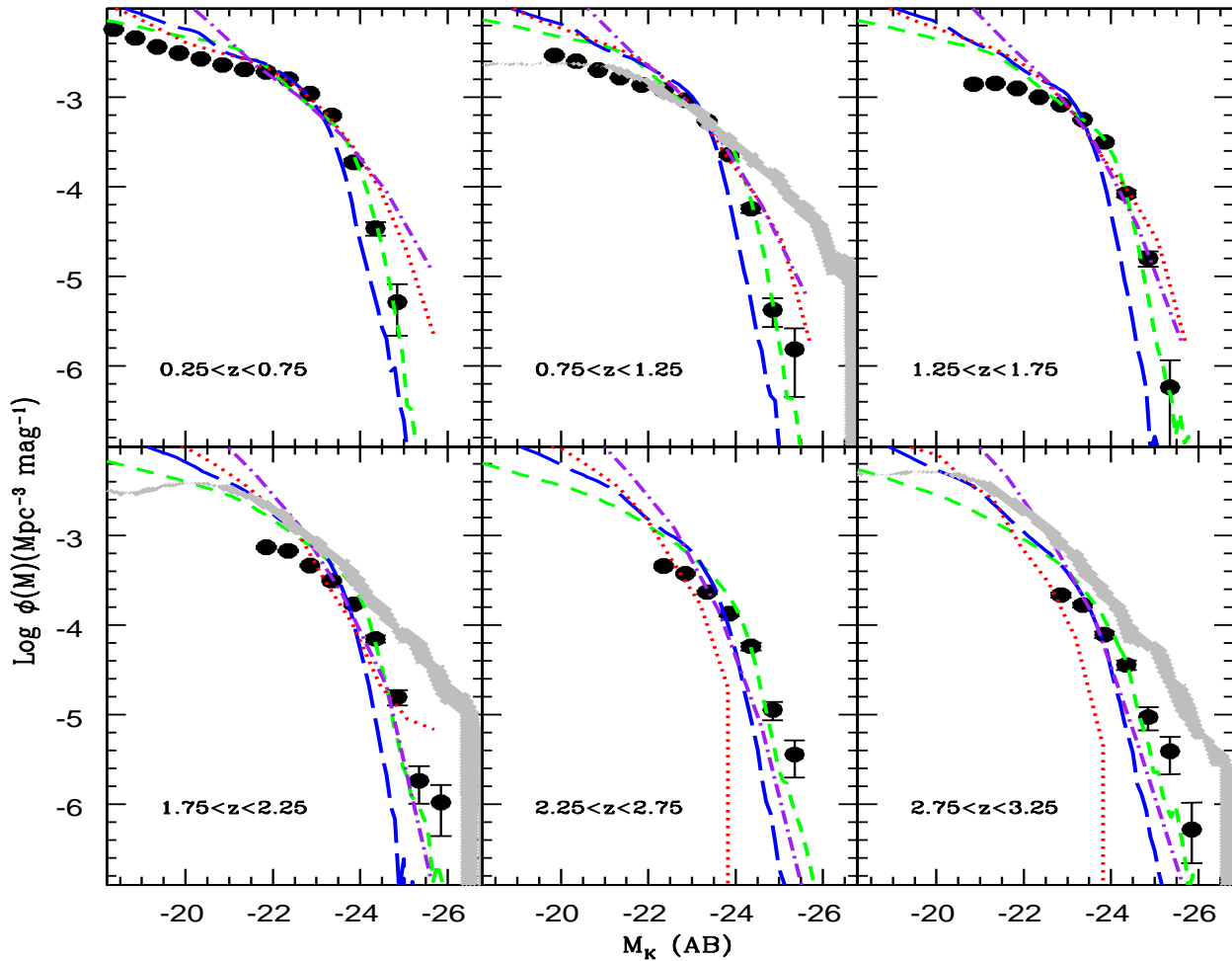


Figure 6. Comparison of our determination of the K -band LF (solid dots) with predictions of theoretical models. Short and long dashed lines are the predictions obtained by Bower et al. (2006) and De Lucia & Blaizot (2007), respectively. The predictions by Monaco et al. (2007) and Menci et al. (2006) are shown with a red dotted curve and purple dot-dashed curve, respectively. The gray area shows the prediction obtained by hydrodynamical simulations (Nagamine et al. 2006; Cen & Ostriker 2006).

tions (Nagamine et al. 2006; Cen & Ostriker 2006). The inclusion of feedback from nuclear accretion has dramatically improved the ability of these models to reproduce the bright end of the LF. However, especially at high redshift, there is still a wide scatter in the predicted number of luminous galaxies produced by the different prescriptions for the physical processes implemented in the various semi-analytical models. On the other hand, hydrodynamical simulations that have yet to incorporate AGN feedback, still systematically over-predict the number of bright/massive galaxies.

Although encouraging, these comparisons show that substantial discrepancies between the models and the data are still present. In particular, all models tend to over-predict the number of low-luminosity galaxies at any redshift. This is probably due to very low star-formation efficiency in real low-mass systems, which is difficult to implement in the models. This problem seems to be less severe in the hydrodynamical simulations, but only at low redshift.

In conclusion, while the overall qualitative agreement between the data and the models is promising, some tension is still clearly present at both low and high luminosities. This suggests that probably some fundamental physical process(es) is(are) still missing in the models, or that the models need to be further fine tuned. This also shows how detailed and accurate observational estimates of the space density of galaxies, in particular at high redshift, can prove to be a very powerful tool for the testing of galaxy-formation models. In the near future we aim to exploit the forthcoming deeper *Spitzer* IRAC and MIPS observations in the UDS to extend the study presented here to the direct derivation of stellar-mass growth and star-formation as a function of cosmic time.

7 ACKNOWLEDGEMENTS

MC, SF and CS would like to acknowledge funding from STFC. RJM, OA would like to acknowledge the funding of the Royal Society. We are grateful to R.C. Bower, K. Nagamine, P. Monaco, F. Fontanot, G. De Lucia and N. Menci for having provided us with the predictions from their latest models. We are also grateful to the staff at UKIRT and Subaru for making these observations possible. We also acknowledge the Cambridge Astronomical Survey Unit and the Wide Field Astronomy Unit in Edinburgh for processing the UKIDSS data.

REFERENCES

- Bershady, M. A., Lowenthal, J. D., & Koo, D. C., 1998, *ApJ*, 505, 50
- Bertin, E., & Arnouts, S., 1996, *A&A Supplement*, 117, 393
- Bolzonella M., Miralles J.-M., & Pelló, R., 2000, *A&A*, 363, 476
- Bolzonella M., Pelló, R., & Maccagni D., 2002, *A&A*, 395, 443
- Bower, R. G., Benson, A. J., Malbon, R., Helly, J. C., Frenk, C. S., Baugh, C. M., Cole, S., & Lacey, C. G., 2006, *MNRAS*, 370, 645
- Bruzual G., Charlot S., 2003, *MNRAS*, 344, 1000
- Calzetti D., Armus L., Bohlin R.C., Kinney A.L., Koornneef J., Storchi-Bergmann T., 2000, *ApJ*, 533, 682
- Caputi, K. I., McLure, R. J., Dunlop, J. S., Cirasuolo, M., Schael, A. M. 2006, *MNRAS*, 366, 609
- Cen, R., & Ostriker, J. P., 2006, *ApJ*, 650, 560
- Cimatti A., et al. 2002, *A&A*, 381, L68
- Ciotti, L., & Ostriker, J. P., 1997, *ApJL*, 487, L105
- Cirasuolo, M., Shankar, F., Granato, G. L., De Zotti, G., & Danese, L., 2005, *ApJ*, 629, 816
- Cirasuolo, M., et al., 2007, *MNRAS*, 380, 585
- Cole, S., Lacey, C. G., Baugh, C. M., & Frenk, C. S., 2000, *MNRAS*, 319, 168
- Cole, S., et al., 2001, *MNRAS*, 326, 255
- Coleman, G. D., Wu, C.-C., Weedman, D. W., 1980, *ApJS*, 43, 393
- Cowie, L. L., Songaila, A., Hu, E. M., Cohen, J. G., 1996, *AJ*, 112, 839
- Croton, D. J., et al., 2006, *MNRAS*, 365, 11
- Daddi, E., et al., 2002, *A&A*, 384, L1
- Daddi E., Cimatti A., Renzini A, Fontana, A, Mignoli M., Pozzetti L., Tozzi P., Zamorani G., 2004, *ApJ*, 617, 746
- Dickinson, M., Papovich, C., Ferguson, H. C., & Budavári, T., 2003, *ApJ*, 587, 25
- De Lucia, G., & Blaizot, J., 2007, *MNRAS*, 375, 2
- Di Matteo, T., Springel, V., & Hernquist, L., 2005, *Nature*, 433, 604
- Drory, N., Bender, R., Feulner, G., Hopp, U., Maraston, C., Snigula, J., Hill, G. J., 2003, *ApJ*, 595, 698
- Drory N., Salvato M., Gabasch A., Bender R., Hopp U., Feulner, G., Pannella, M., 2005, *ApJL*, 619, L131
- Dunlop, J.S., Guiderdoni, B., Rocca-Volmerange, B., Peacock, J.A., Longair, M.S., 1989, *MNRAS*, 240, 257
- Fabian, A. C., 1999, *MNRAS*, 308, L39
- Fazio, G. G., et al., 2004, *ApJS*, 154, 10
- Feulner, G., Bender, R., Drory, N., Hopp, U., Snigula, J., Hill, G. J., 2003, *MNRAS*, 342, 605
- Fontana A., et al., 2004, *A&A*, 424, 23
- Fontana, A., et al., 2006, *A&A*, 459, 745
- Fontanot, F., Monaco, P., Silva, L., & Grazian, A., 2007, *MNRAS*, 382, 903
- Franx, M., et al., 2003, *ApJL*, 587, L79
- Furusawa H. et al., 2008, *ApJS* accepted, [astro-ph/0801.4017](http://arxiv.org/abs/astro-ph/0801.4017)
- Gardner, J. P., Cowie, L. L., & Wainscoat, R. J., 1993, *ApJL*, 415, L9
- Giavalisco, M., et al., 2004, *ApJL*, 600, L93
- Glazebrook, K., Peacock, J. A., Miller, L., & Collins, C. A., 1995, *MNRAS*, 275, 169
- Granato, G. L., Silva, L., Monaco, P., Panuzzo, P., Salucci, P., De Zotti, G., & Danese, L., 2001, *MNRAS*, 324, 757
- Granato, G. L., De Zotti, G., Silva, L., Bressan, A., & Danese, L., 2004, *ApJ*, 600, 580
- Grazian A., et al., 2006, *A&A*, 449, 951
- Kauffmann, G., White, S. D. M., & Guiderdoni, B., 1993, *MNRAS*, 264, 201
- Kauffmann, G., Colberg, J. M., Diaferio, A., & White, S. D. M., 1999a, *MNRAS*, 303, 188
- Kauffmann, G., Colberg, J. M., Diaferio, A., & White, S. D. M., 1999b, *MNRAS*, 307, 529
- Kinney, A. L., Calzetti, D., Bohlin, R. C., McQuade, K., Storchi-Bergmann, T., Schmitt, H. R., 1996, *ApJ*, 467, 38
- Kochanek, C. S., et al., 2001, *ApJ*, 560, 566
- Lawrence, A., et al., 2007, *MNRAS*, 379, 1599
- Lilly, S. J., Longair, M.S., 1984, *MNRAS*, 211, 833
- Lonsdale C.J., et al. 2003, *PASP*, 115, 897
- Lonsdale C.J., et al. 2004, *ApJS*, 154, 54
- Madau P., 1995, *ApJ*, 441, 18
- Marshall, H. L., Tananbaum, H., Avni, Y., Zamorani, G., 1983, *ApJ*, 269, 35
- McLeod, K. K., & Rieke, G. H., 1995, *ApJ*, 441, 96
- Menci, N., Cavaliere, A., Fontana, A., Giallongo, E., & Poli, F., 2002, *ApJ*, 575, 18
- Menci, N., Fontana, A., Giallongo, E., Grazian, A., & Salimbeni, S., 2006, *ApJ*, 647, 753
- Mignoli, M., et al., 2005, *A&A*, 437, 883
- Mobasher B., et al., 2007, *ApJS*, 172, 117
- Monaco, P., Fontanot, F., & Taffoni, G., 2007, *MNRAS*, 375, 1189
- Moustakas, L. A., Davis, M., Graham, J. R., Silk, J., Peterson, B. A., & Yoshii, Y., 1997, *ApJ*, 475, 445
- Nagamine, K., Cen, R., & Ostriker, J. P., 2000, *ApJ*, 541, 25
- Nagamine, K., Fukugita, M., Cen, R., & Ostriker, J. P., 2001, *MNRAS*, 327, L10
- Nagamine K., Ostriker J. P., Fukugita M., Cen R., 2006, *ApJ*, 653, 881
- Oke, J. B., & Gunn, J. E., 1983, *ApJ*, 266, 713
- Pérez-González, P. G., et al., 2008, *ApJ*, 675, 234
- Perlmutter, S., et al., 1998, *Nature*, 391, 51
- Poggianti, B. M., 1997, *A&AS*, 122, 399
- Pozzetti, L., et al., 2003, *A&A*, 402, 837
- Pozzetti, L., et al., 2007, *A&A*, 474, 443
- Riess, A. G., et al., 1998, *AJ*, 116, 1009
- Rix, H.-W., et al., 2004, *ApJS*, 152, 163
- Saracco, P., Giallongo, E., Cristiani, S., D'Odorico, S., Fontana, A., Iovino, A., Poli, F., & Vanzella, E., 2001, *A&A*, 375, 1
- Saracco, P., et al., 2006, *MNRAS*, 367, 349
- Schmidt, M., 1968, *ApJ*, 151, 393
- Scoville, N., et al., 2007, *ApJS*, 172, 1
- Sekiguki K., et al., 2005, in Renzini A. & Bender R., ed., *Multiwavelength mapping of galaxy formation and evolution*. Springer-Verlag, Berlin, p82
- Silk, J., & Rees, M. J., 1998, *A&A*, 331, L1
- Simpson C., et al., 2006a, *MNRAS*, 372, 741
- Simpson C., et al., 2006b, *MNRAS*, 373, L21
- Somerville, R. S., Primack, J. R., & Faber, S. M., 2001, *MNRAS*, 320, 504
- Spergel, D. N., et al., 2003, *ApJS*, 148, 175
- Spergel, D. N., et al., 2007, *ApJS*, 170, 377
- Springel, V., & Hernquist, L., 2003, *MNRAS*, 339, 289
- Springel, V., et al., 2005, *Nature*, 435, 629
- Surace J., et al. 2005, Technical report, The SWIRE Data release 2, <http://swire.ipac.caltech.edu/swire/astronomers.html>

Tegmark, M., et al., 2004, *Phys. Rev. D*, 69, 103501
Warren, S. J., et al., 2007, *MNRAS*, 375, 213
White, S. D. M., & Frenk, C. S., 1991, *ApJ*, 379, 52